

Supporting Information

Multifunctional black phosphorus pressure sensors with bending angle and direction recognition characteristics

Jiangtao Chen,^{a*} Guobin Ma,^a Xinyi Wang,^a Tiancheng Song,^a Yirun Zhu,^a Shuangju Jia,^a
Xuqiang Zhang,^a Yun Zhao,^a Jianbiao Chen,^a Bingjun Yang,^b and Yan Li^a

^aKey Laboratory of Atomic and Molecular Physics & Functional Materials of Gansu Province, College of Physics and Electronic Engineering, Northwest Normal University, Lanzhou 730070, China

^bLaboratory of Clean Energy Chemistry and Materials, State Key Laboratory of Solid Lubrication, Lanzhou Institute of Chemical Physics, Chinese Academy of Sciences, Lanzhou 730000, China

The file includes:

Figure S1 (a) the photograph of the vacuum-filtered BP film, (b) surface SEM observation of black phosphorus film.

Figure S2 BP dispersion in NMP (a) and Tyndall phenomenon (b).

Figure S3 UV-vis-NIR absorption spectrum of BP dispersion in NMP.

Figure S4 SAED pattern of BP nanoflakes.

Figure S5 Lateral size distribution of BP nanoflakes.

Figure S6 AFM topography of BP (a), and corresponding height profiles along the white lines (b) and (c).

Figure S7 The photograph of the interdigital electrode fabricated by thermal-evaporated copper film on flexible PI substrate.

Figure S8 The resistance changes of the device under different applied pressures.

Figure S9 Response and recovery curve of the sensor under the pressure of 40 kPa.

Figure S10 The stability test of the sensor over 1400 loading-unloading cycles under pressure of 24 kPa.

Figure S11 The sensing curves of handwriting process with numbers 0-9 (a, b) and English letters A-Z (c, d, e and f). The handwriting process is performed by volunteer.

Figure S12 Schematic diagram of remote monitoring, collecting current change by a multimeter and showing on a mobile phone in real time via a Bluetooth module.

Figure S13 The durability of the sensor under bending cycling test with angles of 10 and 25°.

Figure S14 Photograph of BP-based pressure sensor array that fixed on a piece of glass.

Figure S15 Photograph of our home-made $\text{Cu}_2\text{ZnSn}(\text{S},\text{Se})_4$ thin film solar cell arrays.

Figure S16 Current density-voltage (J-V) characteristics of the solar cell based on $\text{Cu}_2\text{ZnSn}(\text{S},\text{Se})_4$ under calibrated AM 1.5G illumination generated by an AAA-class solar simulator (Oriel Sol3A 94023A, from Newport), current-voltage (I-V) curves were recorded on a Keithley 4200-SCS semiconductor measurement system.

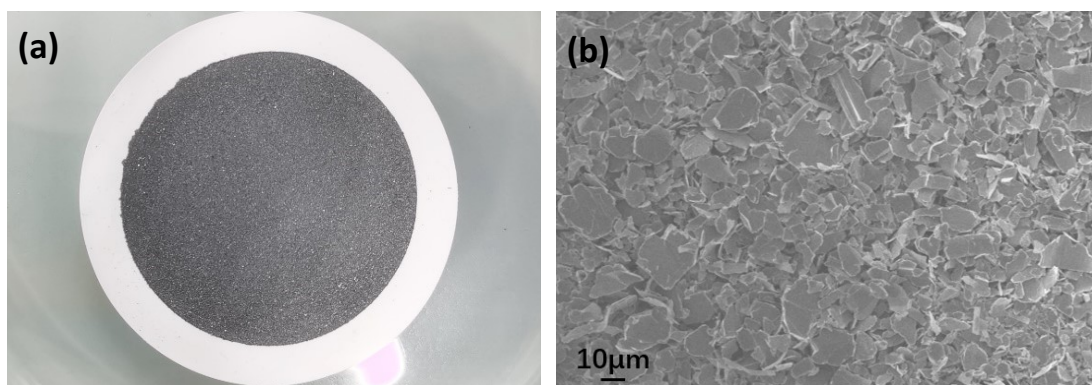


Figure S1 (a) the photograph of the vacuum-filtered BP film, (b) surface SEM observation of black phosphorus film.

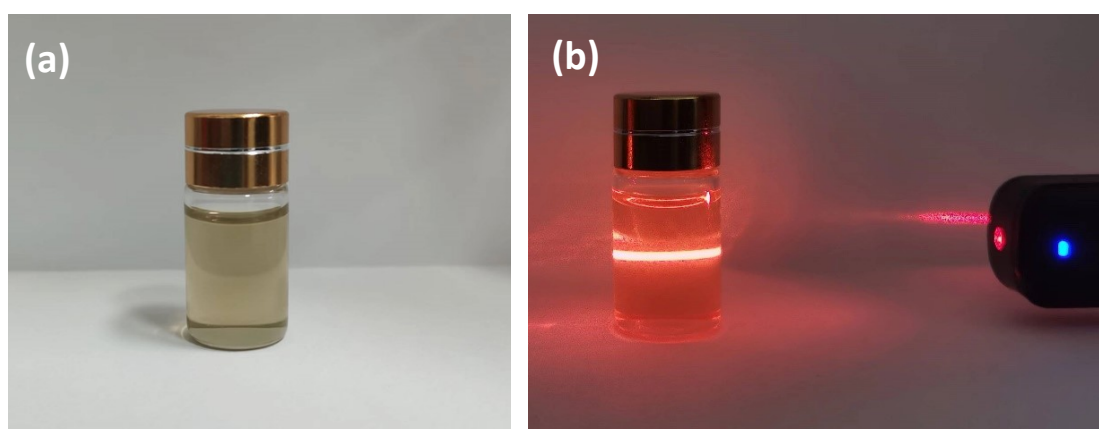


Figure S2 BP dispersion in NMP (a) and Tyndall phenomenon (b).

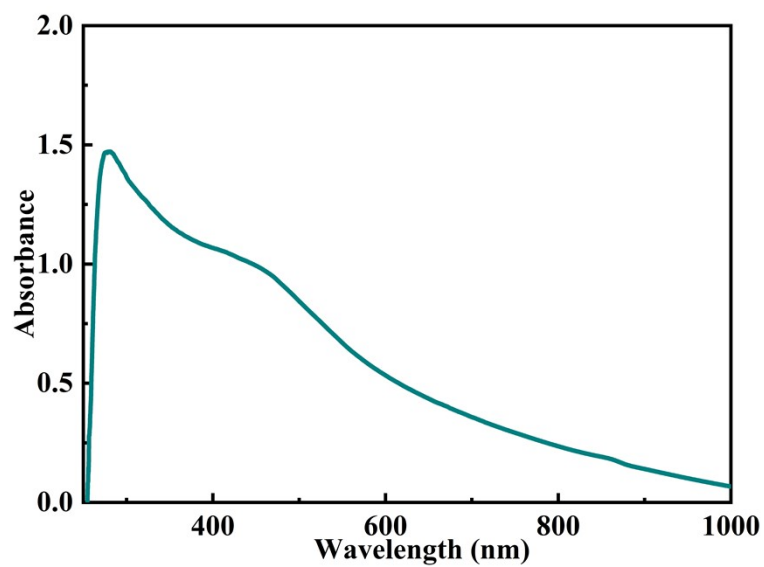


Figure S3 UV-vis-NIR absorption spectrum of BP dispersion in NMP.

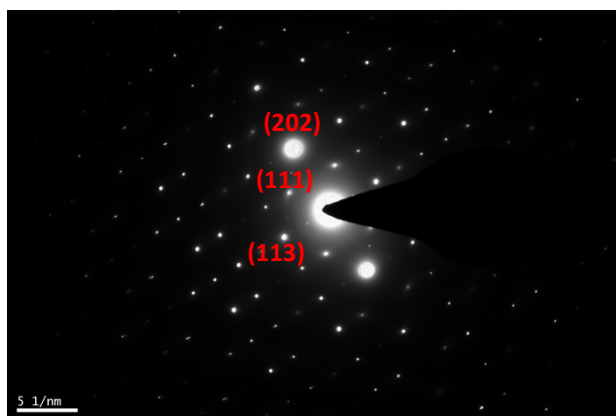


Figure S4 SAED pattern of BP nanoflakes.

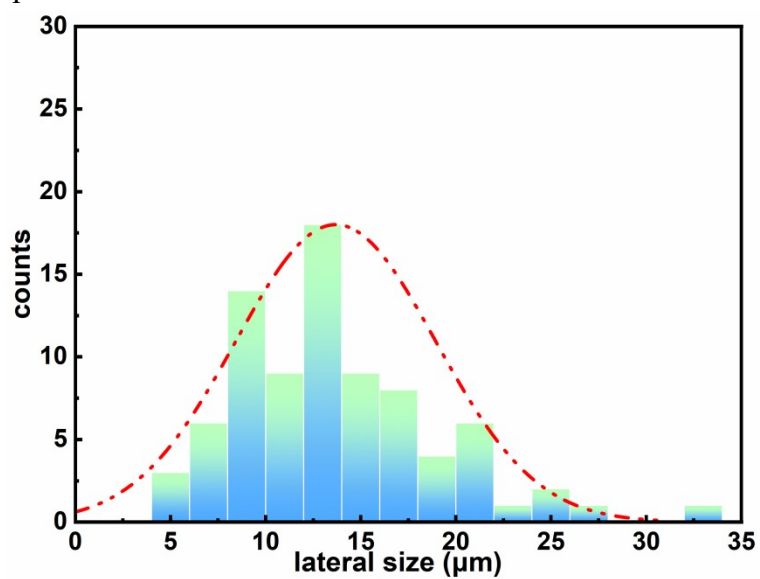


Figure S5 Lateral size distribution of BP nanoflakes.

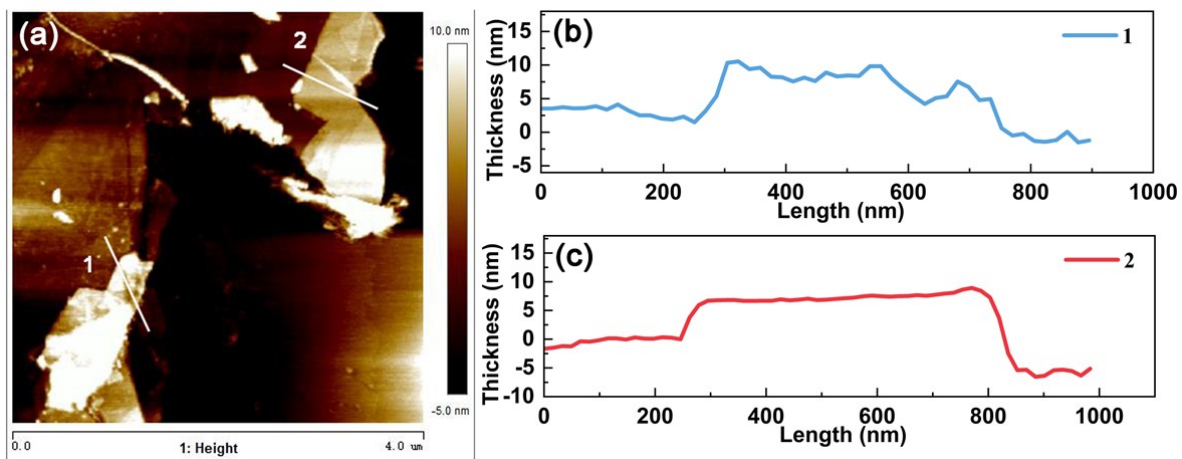


Figure S6 AFM topography of BP (a), and corresponding height profiles along the white lines (b) and (c).

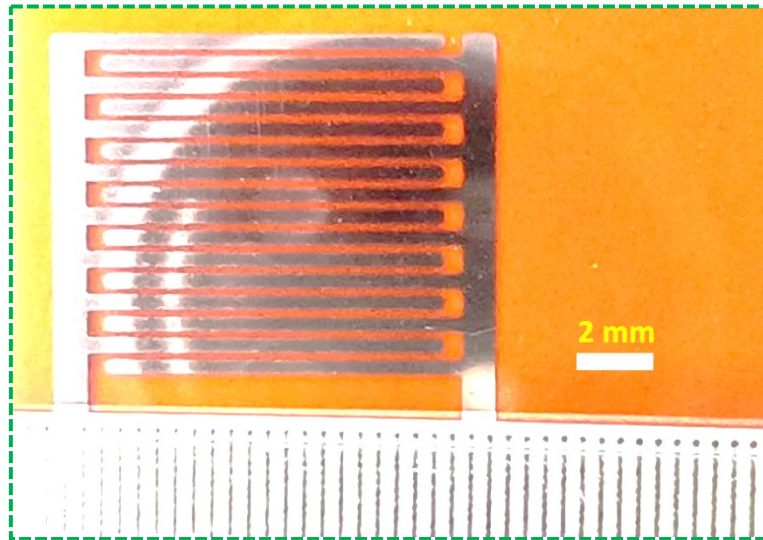


Figure S7 The photograph of the interdigital electrode fabricated by thermal-evaporated copper film on flexible PI substrate.

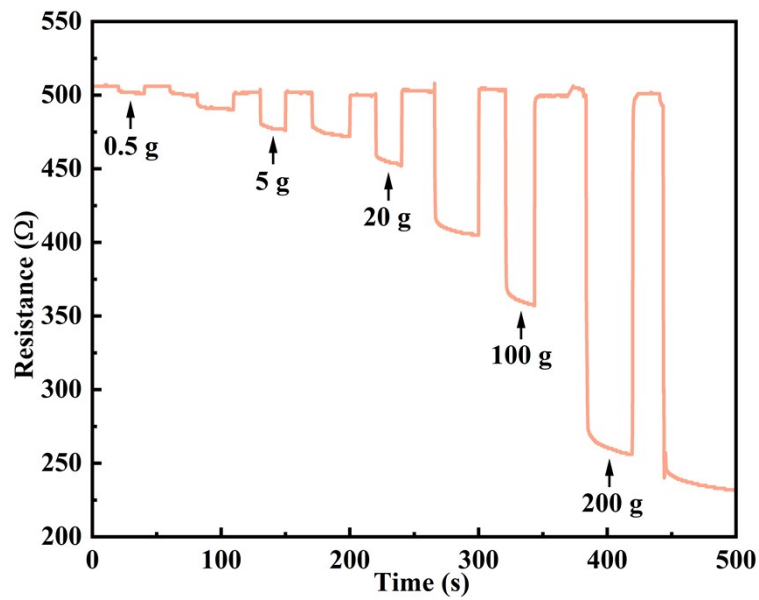


Figure S8 The resistance changes of the device under different applied pressures.

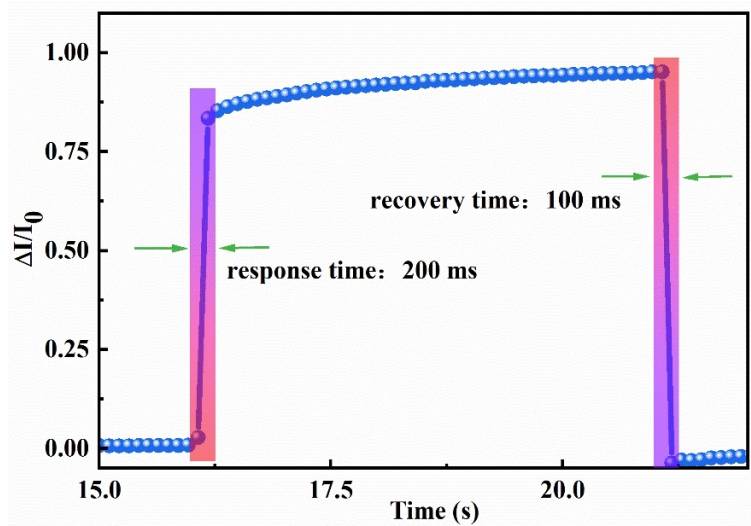


Figure S9 Response and recovery curve of the sensor under the pressure of 40 kPa.

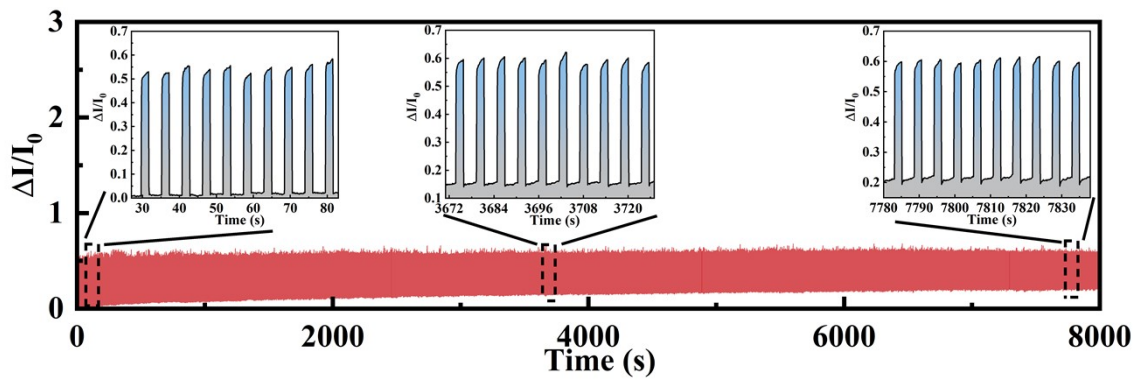


Figure S10 The stability test of the sensor over 1400 loading-unloading cycles under pressure of 24 kPa.

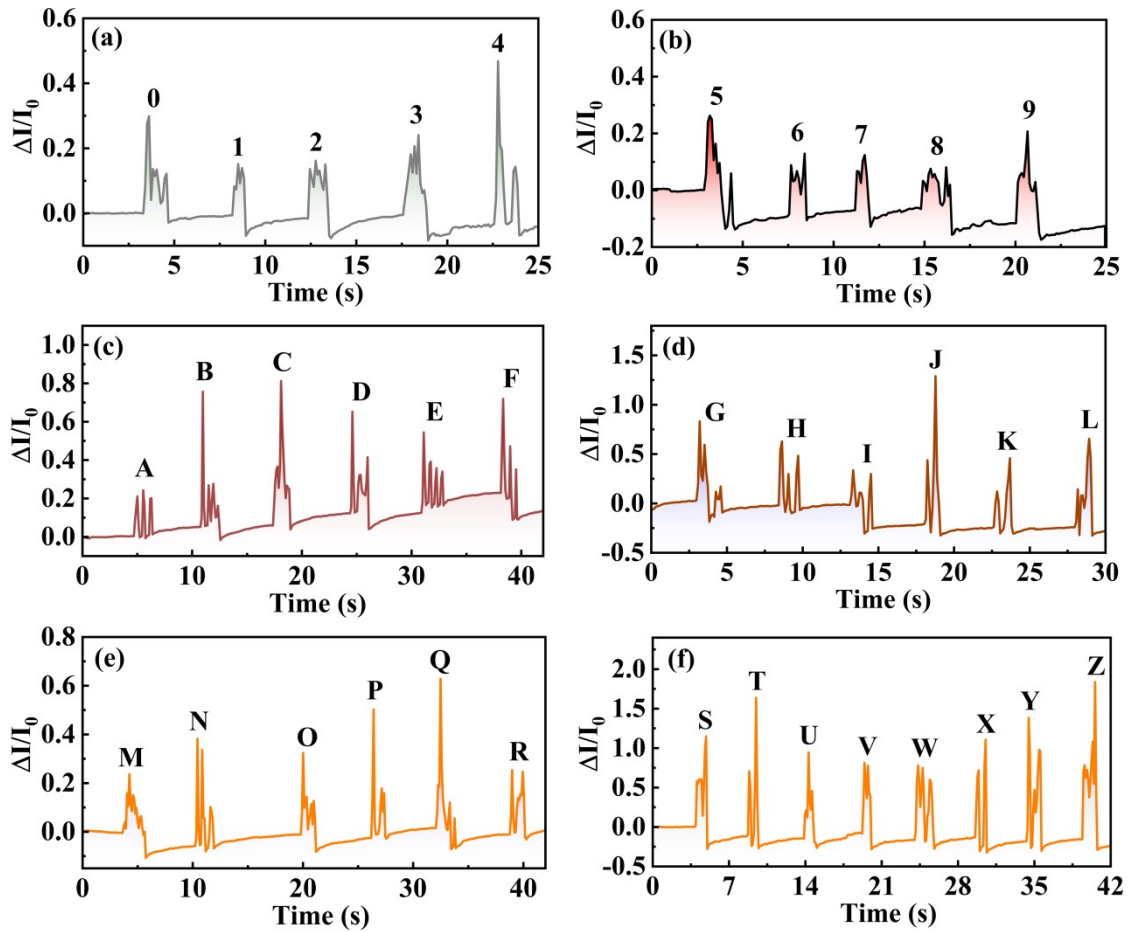


Figure S11 The sensing curves of handwriting process with numbers 0-9 (a, b) and English letters A-Z (c, d, e and f). The handwriting process is performed by volunteer.

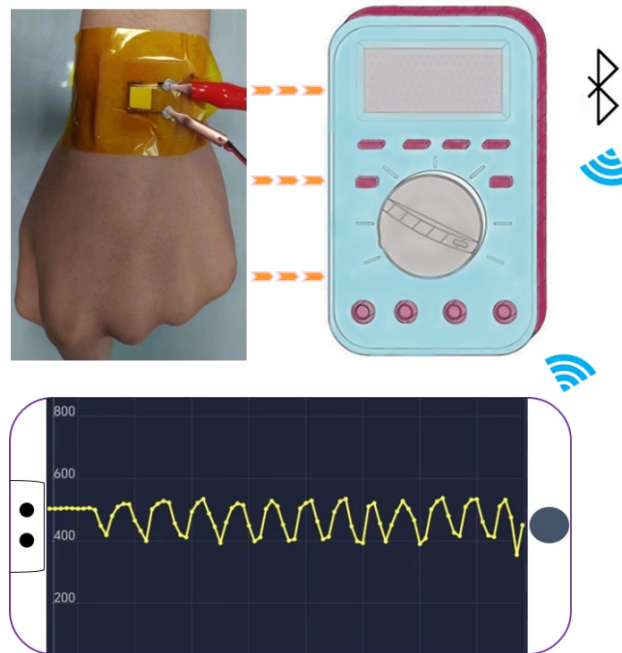


Figure S12 Schematic diagram of remote monitoring, collecting current change by a multimeter and showing on a mobile phone in real time via a Bluetooth module.

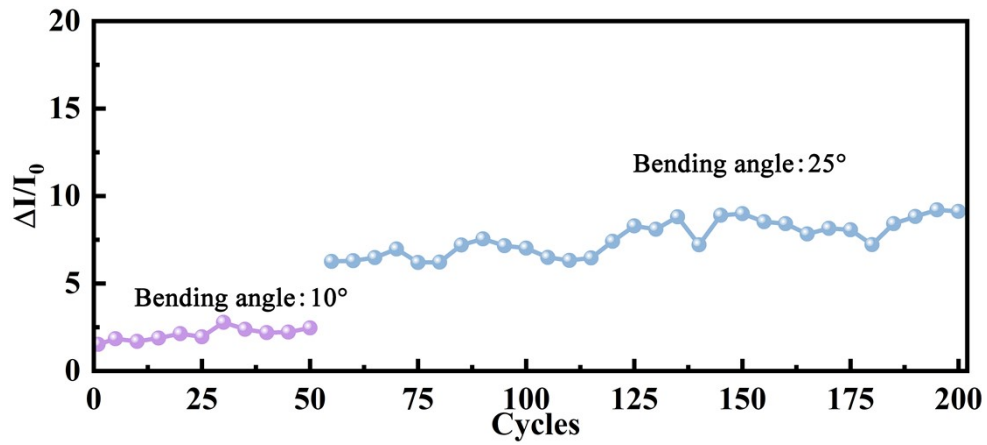


Figure S13 The durability of the sensor under bending cycling test with angles of 10 and 25°.

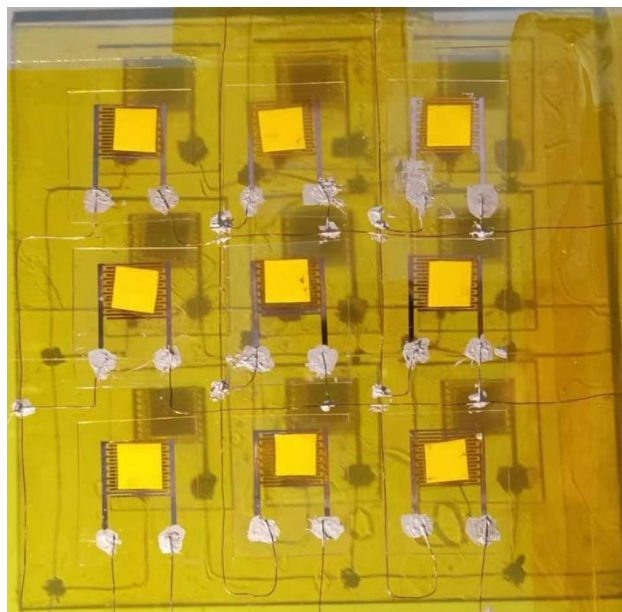


Figure S14 Photograph of BP-based pressure sensor array that fixed on a piece of glass.

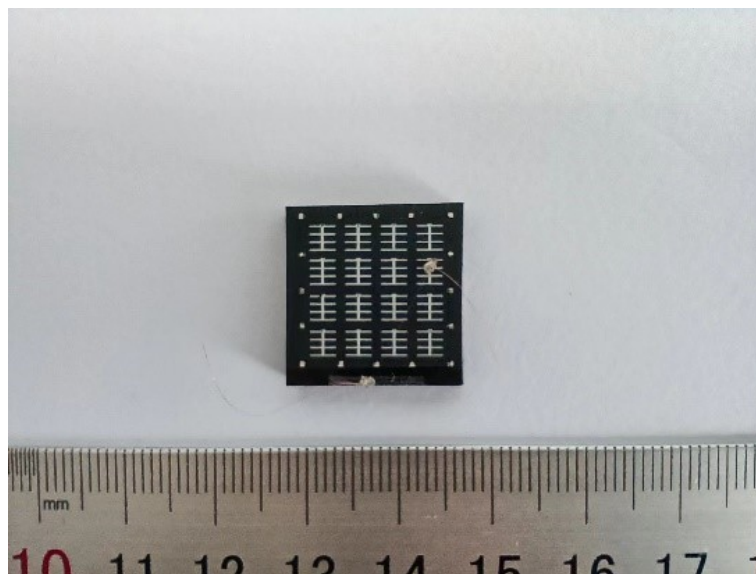


Figure S15 Photograph of our home-made $\text{Cu}_2\text{ZnSn}(\text{S,Se})_4$ thin film solar cell arrays.

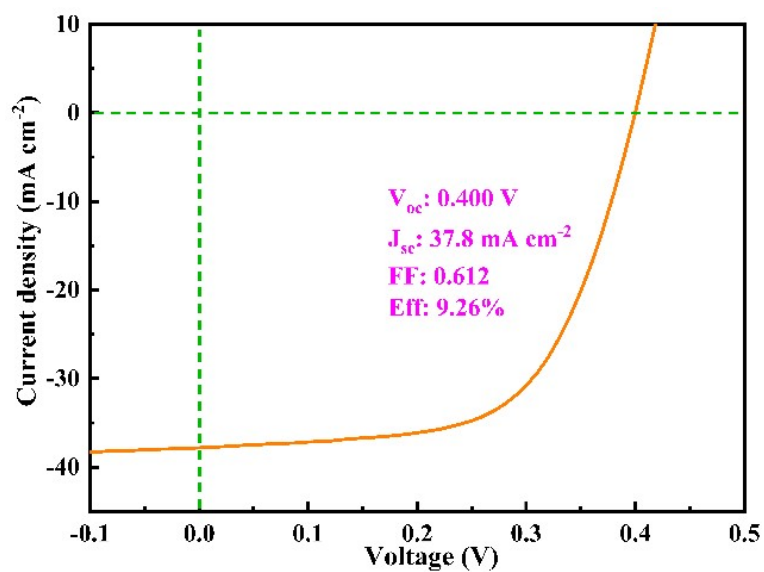


Figure S16 Current density-voltage (J-V) characteristics of the solar cell based on $\text{Cu}_2\text{ZnSn}(\text{S},\text{Se})_4$ under calibrated AM 1.5G illumination generated by an AAA-class solar simulator (Oriel Sol3A 94023A, from Newport), current-voltage (I-V) curves were recorded on a Keithley 4200-SCS semiconductor measurement system.